Raman spectroscopic evidence for the charge disproportionation in a quasi-two-dimensional organic conductor θ-(BDT-TTP)$_2$Cu(NCS)$_2$

J. Ouyang and K. Yakushi
Institute for Molecular Science, Myodaiji, Okazaki, Aichi 444-8585, Japan

Y. Misaki and K. Tanaka
Department of Molecular Engineering, Kyoto University, Kyoto 606-8501, Japan

(Received 31 July 2000; published 5 January 2001)

We present spectroscopic evidence for the charge disproportionation in the crystal θ-(BDT-TTP)$_2$Cu(NCS)$_2$ (BDT-TTP=2,5-bis(1′,3′-dithiol-2′-ylidene)-1,3,4,6-tetrathia-pentalene). θ-(BDT-TTP)$_2$Cu(NCS)$_2$ is a highly correlated organic conductor with a quasi-two-dimensional electronic structure. In the electrical resistance of this compound, we found a second-order phase transition at 250 K. Below this phase-transition temperature, the optical absorption in the midinfrared region exhibits a high-frequency shift, and the Raman-active C=C stretching modes ν_2, ν_3, and ν_4, which are sensitive to the charge on BDT-TTP, split into 12 bands at 5 K. Based on the excitation-light dependence of the Raman spectrum, we propose that a disproportionation of charge occurs below the phase-transition temperature.

DOI: 10.1103/PhysRevB.63.054301 PACS number(s): 71.30.+h, 78.30.−j, 78.30.Jw, 78.20.Ci

In highly correlated organic conductors, the important role of the intermolecular (intersite) Coulomb interaction has recently attracted attention.[1,2] Owing to the strong intermolecular Coulomb interaction, the charge localization and ordering has been experimentally suggested for several organic conductors. Charge disproportionation was found by Hiraki and Kanoda in the quasi-one-dimensional conductor (DI-DCNOI)$_2$Ag.[2,3] In this compound, the two equivalently charged molecules in a unit cell are separated into charge-rich and charge-poor molecules at 220 K. Hiraki and Kanoda propose that the nonequivalent charge is ordered like a Wigner crystal. In the case of quasi-two-dimensional organic conductors, the charge ordering is found by NMR in α-(BEDT-TTF)$_2$I$_3$. (Ref. 4) and in the low-temperature phase of θ-(BEDT-TTF)$_2$RbZn(SCN)$_4$.[5] Nakamura, *et al.* pointed out the possibility of charge disproportionation in θ-(BEDT-TTF)$_2$CsZn(SCN)$_4$ from the analysis of the principal axes of the electron-spin-resonance g value.[6] Recently, Seo published a theoretical study on the charge ordering in BEDT-TTF salts in the framework of a mean-field theory.[7]

The BDT-TTP molecule (see Fig. 1) and its derivatives have yielded many stable organic metals.[8–10] Among these metals, θ-(BDT-TTP)$_2$Cu(NCS)$_2$ is an exceptionally nonmetallic compound even at room temperature, although the band calculation predicts a closed Fermi surface. This compound has the molecular arrangement of a so-called θ type, in which the molecules are arranged like a herringbone without dimerized structure. In this compound, we found a phase transition in the electrical resistivity which was accompanied by a dramatic change in the reflection and Raman spectra. In this paper, we show spectroscopic evidence for the disproportionation of charge below the phase-transition temperature of θ-(BDT-TTP)$_2$Cu(NCS)$_2$.

The crystals of θ-(BDT-TTP)$_2$Cu(NCS)$_2$ were prepared by following an electrochemical method described elsewhere.[11] The crystals exhibited polymorphism. The θ-type crystal has a needlelike shape elongated along the b axis with typical dimensions of $1.0\times0.2\times0.01\,\mathrm{mm}^3$. The well-developed crystal face was (100) with a smooth and shiny surface. The crystal face and the crystallographic axes were determined by the x-ray diffraction method using an Enraf-Nonius CAD4 diffractometer. The electrical resistance was measured along the b axis by a four-probe method using a Quantum Design physical properties measurement system. The electrical contact with 20 μm gold wire was made with a silver paint (Du Pont 4922 N). The polarized reflection spectrum was measured on the (100) face with the polarization parallel to the b and c axes using a microspectroscopic method. The spectrum was measured in the range of 600–30 000 cm^{-1} at room temperature and 600–7000 cm^{-1} at low temperature. The detailed experimental method is described elsewhere.[12] The Raman spectrum was measured on a Renishaw Ramascope System-1000 with a backscattering geometry. The scattered light was analyzed by a polarization

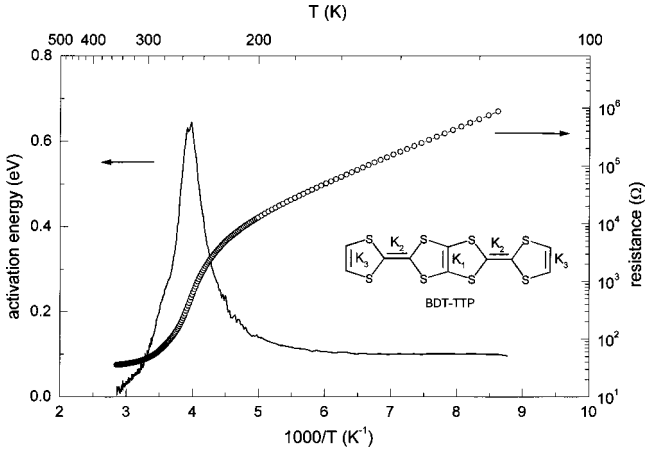

FIG. 1. Temperature-dependent resistances and activation energy of θ-(BDT-TTP)$_2$Cu(NCS)$_2$ single crystal along the b axis from 350 to 102 K. The resistivity at room temperature is ~30 mΩ cm. The inset shows the structural formula of the BDT-TTP molecule.

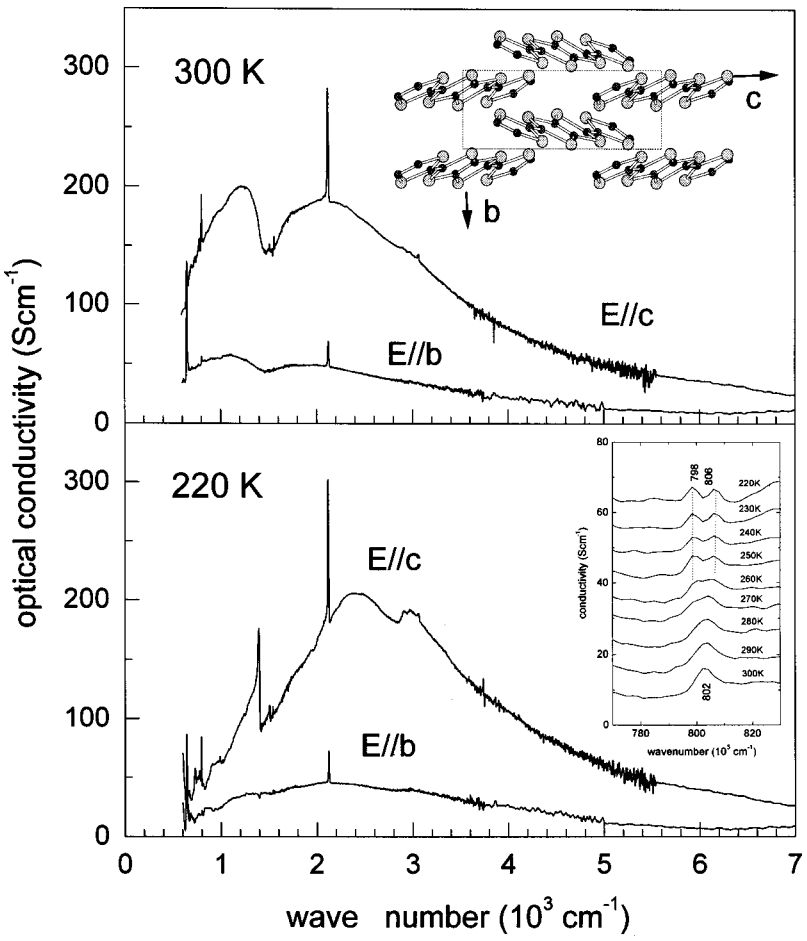

FIG. 2. Optical conductivity spectra of θ-(BDT-TTP)$_2$Cu(NCS)$_2$ with polarization along the *b* and *c* axes above (top panel) and below (bottom panel) the phase-transition temperature. The inset of the top panel shows the arrangement of BDT-TTP molecules projected along the *a* axis and that of the bottom panel shows the infrared spectra of the C—S stretching region.

filter with an extinction ratio of 10^{-4}. For example, the $a^*(c,b)a^*$ spectrum denotes an experimental condition in which the laser is polarized along the *c* axis, the analyzer is polarized along the *b* axis, and the wave vector is parallel to the a^* axis. We used He-Ne and Ar^+ lasers with respective wavelengths at 632.8 and 514.5 nm. The intensity at the crystal face was less than 1.5 mW for the He-Ne laser and less than 0.5 mW for the Ar^+ laser. Higher laser power results in photo damage to the sample. The cryostat system for this spectrometer is described elsewhere.[13]

θ-(BDT-TTP)$_2$Cu(NCS)$_2$ belongs to the mono-clinic system with space group Cc.[11] Just like the θ-(BEDT-TTF)$_2MM'$(SCN)$_4$ (M=Rb, CS; M'=Co, Zn),[14,15] the unit cell contains two conducting layers separated by the counter anion. Each conducting layer is parallel to the (100) plane and involves two BDT-TTP molecules connected by a glide plane (see Fig. 2). The four molecules in the unit cell are therefore crystallographically equivalent. Based on the molecular arrangement in the conducting layer, the two-dimensional tight-binding band is yielded by the following equation:

$$E(k_b,k_c)=2t_b b\cos(k_b b)\pm\sqrt{2[1+\cos(k_c c)][t^2{}_{p1}+t^2{}_{p2}+2t_{p1}t_{p2}\cos(k_b b)]}. \quad (1)$$

The transfer integrals were estimated as $t_b=-0.041$, $t_{p1}=-0.086$, and $t_{p2}=-0.091$ eV from the overlap integral of the highest occupied molecular orbital (HOMO) calculated by the extended Hückel method,[11] where t_b is the transfer integral along the *b* axis, and t_{p1} and t_{p2} are those between the molecules related by a glide plane. Equation (1) produces a closed Fermi surface when we use the above transfer integrals. The band calculation requires a metallic state for this compound.

Figure 1 shows the temperature-dependent resistance and activation-energy curves in the cooling process. The resistance was measured at a cooling rate of 0.5 K/min, and no hysteresis was observed in the heating process. The activation energy continuously increased from ~17 meV around 340 K, reached a maximum at ~250 K, decreased to 100 meV around 200 K, and then leveled off below 200 K. We

considered this change to be the second-order phase transition. In the whole temperature range, this compound was a nonmetal. From the θ-type molecular arrangement, we can reasonably accept the relation $|t_b|<|t_{p1}|\approx|t_{p2}|$. Under this restriction, any combination of the transfer integrals yields a closed Fermi surface. Therefore, the nonmetallic property is likely to be ascribed to the correlation effect. Since the crystal structure of this compound resembles the θ-type family of BEDT-TTF salts, an analogous reasoning may be applied to this compound. The phase diagram of the θ-type family of BEDT-TTF salts has been proposed by Mori, Tanaka, and Mori.[15] The electronic phase of the θ-type BEDT-TTF salts is mapped against the dihedral angle θ of the molecular planes in the same conducting layer. The dihedral angle is related to the bandwidth: the larger the dihedral angle θ, the narrower the bandwidth. In this phase diagram, the materials with $\theta>120°$ are nonmetallic in the whole temperature region. The closest compound, θ-$(BEDT\text{-}TTF)_2Cu_2(CN)[N(CN)_2]_2$,[16] has a dihedral angle of 132° and shows an insulator-to-insulator phase transition at approximately 220 K. θ-$(BDT\text{-}TTP)_2Cu(NCS)_2$ with $\theta=134°$ can probably be classified into these highly correlated nonmetallic BEDT-TTF salts.

Figure 2 shows the optical conductivity spectra of the high- and low-temperature phases obtained from the Kramers-Kronig transformation of the polarized reflection spectra. Although the optical conductivity is mainly polarized along the c direction, it also has a spectral weight in the b polarization. This indicates that θ-$(BDT\text{-}TTP)_2Cu(NCS)_2$ is a quasi-two-dimensional system. The strong polarization along the c axis is qualitatively consistent with the relation between the transfer integrals $|t_b|<|t_{p1}|$, $|t_{p2}|$. The broad dip at 1500 cm^{-1} in the $E\|c$ spectrum seems to be a Fano-like antiresonance *via* the electron-molecular vibration (EMV) coupling of the totally symmetric C═C stretching mode.[17] As shown in Fig. 2, a drastic change is observed in the conductivity spectrum below the phase-transition temperature. In the low-temperature phase, the spectral weight below 1500 cm^{-1} is lost in both directions. At the same time, the main peak shifts to 2400 cm^{-1} and a bump appears at 3000 cm^{-1} together with several CH stretching bands. This spectral change is consistent with the broadening of the gap observed in the resistivity experiment. The asymmetric broad phonon band at 1398 cm^{-1} in the $E\|c$ spectrum is characteristic of the EMV-coupled a_g-mode line shape. The appearance of this band in the $E\|c$ spectrum suggests the breaking of the glide-plane symmetry along the c axis. Incidentally, the integrated intensity in this region slightly decreases below the phase transition; for example, the ratio is 0.9 for $E\|b$ and 0.95 for $E\|c$ at 220 K. This decrease of intensity is opposite to the ordinary behavior. This result might suggest that a structural change occurs during the phase transition. The inset of the lower panel of Fig. 2 shows the temperature-dependent $E\|c$ spectrum in the 770–830 cm^{-1} region. This band is assigned to the b_{2u} C-S stretching mode, which splits into two bands below 250 K.

Figure 3 shows the temperature-dependent $a^*(c,c)a^*$ Raman spectrum excited by the 632.8 nm laser in the region of the C═C stretching modes. When the temperature is lowered, the Raman spectrum as well as the reflection spectrum shows a dramatic change. The broad band at 1486 cm^{-1} sharpens continuously along with a remarkable high-frequency shift (see the inset of Fig. 3). At the same time, two broad components appear in the low-frequency tail and form broad humps. At 5 K, the low-frequency hump grows to a strong broadband at 1391 cm^{-1} and the high-frequency one splits into sharp and broad bands at 1442 and 1456 cm^{-1}. The other four sharp peaks appear both in the low- and high-frequency sides of the 1500 cm^{-1} band. Figure 4 shows the $a^*(c,c)a^*$ and $a^*(c,b)a^*$ spectra excited by 632.8 nm, the $a^*(c,c)a^*$ spectrum excited by 514.5 nm, and the spectra of $(BDT\text{-}TTP)_2SbF_6$ and BDT-TTP excited by 632.8 nm. As shown in Fig. 4(e), the BDT-TTP neutral crystal exhibits three strong Raman bands in this region. We conducted a normal coordinate analysis for the in-plane vibrational modes of the BDT-TTP neutral crystal.[18] BDT-TTP has three kinds of nonequivalent C═C bonds: inner ring C═C (K_1), bridging C═C (K_2), and outer ring C═C (K_3) (see the inset of Fig. 1). According to the analysis, the three bands are assigned to the following a_g modes: $K_2(43)+K_3(27)$ for ν_2 at 1555 cm^{-1}, $K_1(44)+K_3(45)$ for ν_3 at 1525 cm^{-1}, and $K_1(36)+K_2(38)$ for ν_4 at 1504 cm^{-1}.[19] Except for the C═C stretching modes, the Raman active mode in this spectral region (1200–1700 cm^{-1}) is the ν_{46} (b_{3g}) in-plane CH bending mode at 1253 cm^{-1}. This means that the Raman bands in this region are ascribed to the C═C stretching modes.

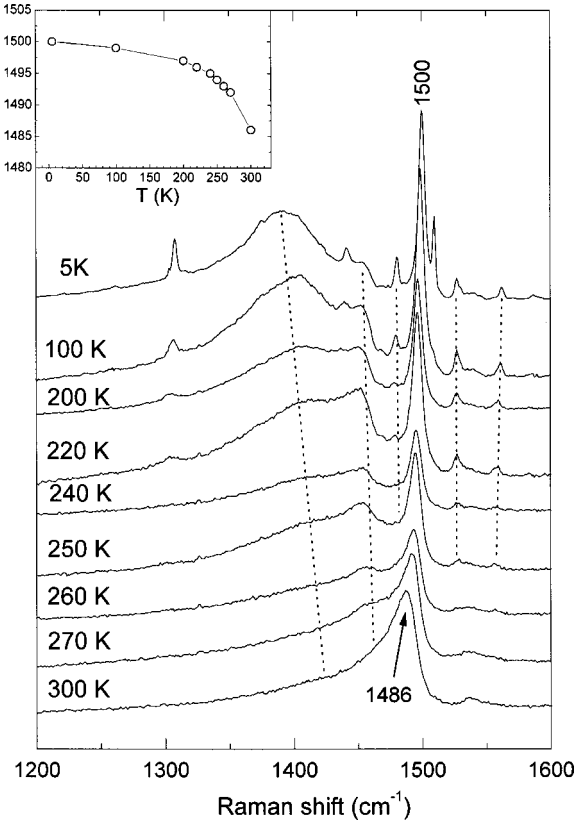

FIG. 3. Evolution of the Raman bands in the region of the C═C stretching modes in θ-$(BDT\text{-}TTP)_2Cu(NCS)_2$. Polarization is (c,c) excited by the He-Ne laser. The inset shows the temperature dependence of the frequency of the ν_4^A mode.

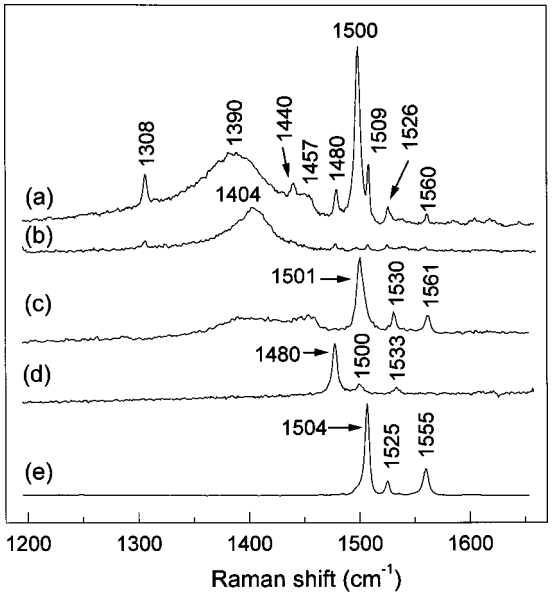

FIG. 4. Polarized (a) $a^*(c,c)a^*$ and (b) $a^*(c,b)a^*$ Raman spectra of θ-(BDT-TTP)$_2$Cu(NCS)$_2$ at 5 K excited by the 632.8 nm laser and (c) $a(c,c)a^*$ spectrum of θ-(BDT-TTP)$_2$Cu(NCS)$_2$ at 5 K excited by the 514.5 nm laser. (d) Polarized $b^*(a,a+c)b^*$ Raman spectrum of metallic (BDT-TTP)$_2$SbF$_6$ crystal excited by the 632.8 nm laser. (e) Polarized $a^*(b,b)a^*$ Raman spectrum of neutral BDT-TTP crystal excited by the 632.8 nm laser.

Let us discuss the factor group analysis of this compound under the space group of Cc. First of all, we neglect the charge-transfer interaction between the two conducting layers separated by the counter anions. Since the unit layer contains two molecules, every intramolecular vibrational mode is twofold degenerate if the intermolecular interaction is weak enough. In the factor group of C_s, the vibrational modes are classified into the crystal modes with an A' and A'' symmetry. The A' mode corresponds to the in-phase molecular vibration, where the molecules connected by the glide plane vibrate in phase with each other. On the other hand, in the A'' mode, the molecules related by symmetry vibrate out of phase. In the latter case, the EMV interaction works strongly through the charge transfer between the molecules in the unit cell, and thus the coupled vibration modulates the electric dipole and polarizability of the unit cell.[20] As is well known in the infrared spectrum of organic conductors, the A'' mode shifts to the low-frequency side depending upon the coupling constant and broadens the linewidth owing to be mixed with the electronically excited state at 2400 cm^{-1}.[21] As shown in Fig. 4(a) the appearance of many Raman bands suggests the splitting of the degenerate modes through an EMV interaction. The A' mode is allowed in (a,a), (b,b), (c,c), and (a,c) polarizations, whereas the A'' mode is allowed in (a,b) and (b,c) polarizations. A comparison between Figs. 4(a) and 4(b) shows that this selection rule is broken for 1480, 1509, 1526, and 1560 bands. Furthermore, the broadbands appear in the (cc) polarization. These results indicate that the glide-plane symmetry is broken at 5 K. If the size of the unit cell is preserved, the observable Raman band is at most 6 because the molecule has three Raman-active C═C stretching modes. Since nine bands are found in the 1320–1580 cm^{-1} region of the (cc) spectrum, we conclude that the unit cell is doubled without preserving the glide-plane symmetry. As a whole, we observe seven sharp bands and five broadbands including the other bands found in the (a,a) and (b,b) spectra. Incidentally, we have looked for the superlattice at 100 K in an x-ray oscillation photograph along the b axis but found no such clear diffraction spots as observed in θ-(BEDT-TTF)$_2$RbCo(SCN)$_4$.[22] As shown in Fig. 3, the spectrum continuously changes below room temperature, and the characteristic feature appears already at 220 K. Thus, the structural change and charge disproportionation are closely related to the mechanism of the second-order phase transition at 250 K.

As shown in Fig. 4(d), (BDT-TTP)$_2$SbF$_6$ shows only three C═C stretching bands, although the unit cell contains two molecules. This is because the six C═C stretching modes are classified into three Raman-active A_g modes and three infrared active A_u modes, owing to the factor group of C_1. The Raman-active modes shown in Fig. 4(d) are EMV-uncoupled modes. When we compare the Raman spectrum of this compound with that of (BDT-TTP)$_2$SbF$_6$, which has the same average charge as BDT-TTP, the 1560 cm^{-1} band is higher in frequency than the highest band at 1533 cm^{-1} of (BDT-TTP)$_2$SbF$_6$. Since the EMV interaction always shifts the coupled mode to the low-frequency side, the doubling of the unit cell and lowering of the symmetry cannot explain this band. However, the high-frequency shift can be reasonably explained by the charge disproportionation such as $(\text{BDT-TTP}^{0.5+})_2 \rightarrow \text{BDT-TTP}^{\delta+} + \text{BDT-TTP}^{(1-\delta)+}$ because the frequencies of the C═C stretching modes are sensitive to the charge on BDT-TTP as shown in Figs. 4(d) and 4(e) and because the 1560 cm^{-1} band is close to the ν_2 mode of BDT-TTP^0. When the spectrum is measured by 514.5 nm light, three sharp bands and two broadbands are enhanced and the other bands are suppressed as shown in Fig. 4(c). The sharp bands at 1501, 1530, and 1561 cm^{-1} resemble the 1504, 1525, and 1555 cm^{-1} bands of BDT-TTP^0, including the intensity ratio. It is difficult to explain this excitation-light dependence by means of the structural change. The characteristic feature can also be explained by the charge disproportionation if we consider that the lowest singlet state of BDT-TTP is found at $19-24\times10^3$ cm^{-1} in the solution spectrum. Based on these two reasons, we conclude that the molecule with an average charge of $+0.5$ shows a disproportionation to a charge-rich (BDT-TTP$^{(1-\delta)+}$) and charge-poor (BDT-TTP$^{\delta+}$) species at 5 K. When the charge disproportionation occurs, the doubled unit layer involves four nonequivalent molecules, which are regarded as two charge-poor and two charge-rich molecules. There is no symmetry relation between the two charge-poor molecules and between the two charge-rich molecules. Therefore, the fourfold degenerate ν_i modes split into two nearly degenerate modes for charge-rich and charge-poor molecules if these molecules do not interact with each other. As a matter of fact, the EMV interaction splits each nearly degenerate mode,[23] and thus the fourfold degenerate ν_i modes split into four, depending upon the coupling constant. A vibrational mode strongly coupled

with the electronic excited state shifts to the low-frequency side and broadens the linewidth. Therefore, the sharp and broad bands are considered the weakly and strongly coupled modes, respectively. Taking account of the 514.5 nm excitation spectrum and the low-frequency shift of a coupled mode, we tentatively assigned the 1560, 1500, 1457, and 1390 cm^{-1} bands to the charge-poor molecule and the 1526, 1509, 1480, 1440, and 1404 cm^{-1} bands to the charge-rich molecule.[24]

Next we will discuss the possible charge separation (asymmetric charge distribution) in a single molecule when the disproportionation occurs. A symmetry breakdown and the charge separation in a molecule has been reported in several molecules containing two TTF moieties[25,26] and two benzoquinone moieties.[27] Since the BDT-TTP molecule consists of two TTF moieties, the hole might be localized in one of the TTF moieties accompanying the distortion of the molecular geometry. In this case, the radical cation has five Raman-active modes, and the Raman-active modes split more than those of the symmetric $BDT\text{-}TTP^{+}$. Even in this case, the maximum number of Raman-active C═C stretching modes are eight, three for a charge-poor symmetric molecule, and five for a charge-rich asymmetric molecule, if the unit cell is not doubled. The appearance of 12 bands again leads to the doubling of the unit cell. The vibrational feature of an asymmetric molecule, which involves charge-rich and charge-poor TTF moieties, is nearly the same as that of the system where the charge-rich and charge-poor BDT-TTF molecules coexist. Therefore, it is difficult to distinguish whether the charge-rich molecule is symmetric or asymmetric, when a charge-poor molecule coexists with the charge-rich molecule.

According to Seo's theory, the separated charge is ordered in three different ways, such as vertical, horizontal, and diagonal stripes, depending upon the parameters, U, V, and t. If we neglect the transfer integral t_b, the interaction works only between the charge-rich (B) and charge-poor (A) molecules in a vertical stripe, whereas there are three types of interaction, such as AA, AB, and BB, in horizontal and diagonal stripes. Recently, Tajima *et al.* calculated the optical conductivity by means of solving the extended Hubbard model by the mean-field approximation and interpreted the optical spectra of θ-$(BEDT\text{-}TTF)_2MM'(SCN)_4$ (MM' = CsZn, RbCo, RbZn).[28] They proposed that the optical-conductivity spectrum in the midinfrared region could be used as a fingerprint to determine the ordering pattern. In the crystal of θ-$(BEDT\text{-}TTF)_2RbCo(SCN)_4$, for example, a single broad electronic band splits into three resolved bands below the phase-transition temperature. These three bands correspond to the charge-transfer transitions in the AA, AB, and BB pairs. Within this interpretation, Tajima *et al.* assumed that the ordering pattern of θ-$(BEDT\text{-}TTF)_2RbCo(SCN)_4$ was the horizontal stripe below the phase transition. In θ-$(BDT\text{-}TTP)_2Cu(NCS)_2$, the low-temperature optical conductivity in the infrared region appears to be a single peak as shown in Fig. 2. If we follow Tajima's proposal, the separated charge forms a vertical stripe along the b axis after the phase transition. This model is consistent with the breakdown of the glide-plane symmetry.

In conclusion, we found a phase transition that accompanies a charge disproportionation in the quasi-two-dimensional organic conductor θ-$(BDT\text{-}TTP)_2Cu(NCS)_2$. The charge disproportionation is proved by the low-temperature Raman spectrum in the C═C stretching region. In contrast to the first-order phase transition in θ-$(BEDT\text{-}TTF)_2RbZn(SCN)_4$, which also shows a charge disproportionation below the phase-transition temperature, $(BDT\text{-}TTP)_2Cu(NCS)_2$ shows a second-order phase transition.

We acknowledge Dr. K. Yamamoto of IMS for a fruitful discussion on the interpretation of the Raman spectrum. This research was partly supported by a Grant-in-Aid for Scientific Research on Priority Areas (B) of Molecular Conductors and Magnets (Area No. 730/Grant No. 11224212) from the Ministry of Education, Science, Sports, and Culture of Japan.

[1] F. Mila, Phys. Rev. B **52**, 4788 (1995).
[2] K. Hiraki and K. Kanoda, Phys. Rev. Lett. **80**, 4737 (1998).
[3] K. Kanoda, K. Miyagawa, A. Kawamoto, and K. Hiraki, J. Phys. IV **9**, 353 (1999).
[4] Y. Takano, K. Hiraki, T. Takahashi, M. Yamamoto, and T. Nakamura (private communication).
[5] K. Miyagawa, A. Kawamoto, and K. Kanoda, Phys. Rev. B **62**, R7679 (2000).
[6] T. Nakamura, W. Minagawa, R. Kinami, and T. Takahashi, J. Phys. Soc. Jpn. **69**, 504 (2000).
[7] H. Seo, J. Phys. Soc. Jpn. **69**, 805 (2000).
[8] Y. Misaki, H. Nishikawa, K. Kawakami, S. Koyanagi, T. Yamabe, and M. Shiroo, Chem. Lett. **1992**, 2321.
[9] Y. Misaki, T. Matsui, K. Kawakami, H. Nishikawa, T. Yamabe, and M. Shiroo, Chem. Lett. **1993**, 1337.
[10] T. Mori, T. Kawamoto, Y. Misaki, K. Kawamoto, H. Fujiwara, T. Yamabe, H. Mori, and S. Tanaka, Mol. Cryst. Liq. Cryst. Sci. Technol., Sect. A **284**, 271 (1996).
[11] Y. Misaki, T. Kochi, M. Taniguchi, H. Fujiwara, T. Matsui, T. Yamabe, K. Tanaka, T. Mori, T. Kawamoto, M. Aragaki, H. Mori, and S. Tanaka (unpublished).
[12] J. Ouyang, K. Yakushi, Y. Misaki, and K. Tanaka, J. Phys. Soc. Jpn. **67**, 3191 (1998).
[13] J. Ouyang, J. Dong, K. Yakushi, K. Takimiya, and T. Otsubo, J. Phys. Soc. Jpn. **68**, 3708 (1999).
[14] H. Mori, S. Tanaka, T. Mori, A. Kobayshi, and H. Kobayashi, Bull. Chem. Soc. Jpn. **71**, 797 (1998).
[15] H. Mori, S. Tanaka, and T. Mori, Phys. Rev. B **57**, 12 023 (1998).
[16] T. Komatsu, H. Sato, T. Nakamura, N. Matsukawa, H. Yamochi, G. Saito, M. Kusunoki, K. Sakaguchi, and S. Kagoshima, Bull. Chem. Soc. Jpn. **68**, 2233 (1995).
[17] In the factor group C_s, the antiphase coupled vibration of a_g modes produces the unit-cell dipole only along the b axis. Actually, however, the dip in the $E\|c$ spectrum is larger than that

of $E \| b$. The breakdown of this kind of selection rule is observed also in θ-(BEDT-TTF)$_2$CsCo(SCN)$_4$ [K. Yamamoto and K. Yakushi (unpublished)]. The symmetry may be broken already at room temperature due to the correlation effect.

[18] J. Ouyang, K. Yakushi, Y. Misaki, and K. Tanaka (unpublished).

[19] The numerical value in parentheses denotes the percentage of each bond stretching.

[20] M. Meneghetti, R. Bozio, and C. Pecile, J. Phys. (Paris) **47**, 1377 (1986).

[21] A large coupling constant was calculated by Taniguchi *et al.* for the C═C stretching mode of the bridging C═C bond of BDT-TTP. See M. Taniguchi, Y. Misaki, and K. Tanaka, Solid State Commun. **114**, 75 (2000).

[22] In the case of θ-(BEDT-TTF)$_2$RbCo(SCN)$_4$, clear diffraction spots for the superlattice were detected at 100 K in the imaging plate system for x-ray diffraction.

[23] A. Girlando, R. Bozio, C. Pecile, and J. B. Torrance, Phys. Rev. B **26**, 2306 (1982).

[24] The 1526 cm^{-1} band has a shoulder at ~1530 cm^{-1}, which appears as a peak in the $(b, b+c)$ spectrum along with the 1526 cm^{-1} band.

[25] K. Lahlil, A. Moradpour, C. Bowlas, F. Menou, P. Cassoux, J. Bonvoisin, J-P. Launay, G. Dive, and D. Dehareng, J. Am. Chem. Soc. **117**, 9995 (1995).

[26] K. Pokhondnia, P. Cassoux, J. Bonvoisin, A. Mlayah, L. Brossard, S. Frenzel, and K. Mullen, J. Phys. Chem. B **101**, 3665 (1997).

[27] S. F. Rak and L. L. Miller, J. Am. Chem. Soc. **114**, 1388 (1992).

[28] H. Tajima, S. Kyoden, H. Mori, and S. Tanaka (private communication).